A Review of Propulsion, Power, and Control Architectures for Insect-Scale Flapping-Wing Vehicles

E. Farrell Helbling[1]
John A. Paulson School of Engineering and Applied Sciences,
Wyss Institute for Biologically Inspired Engineering,
Harvard University,
Cambridge, MA 02138
e-mail: ehelbling@seas.harvard.edu

Robert J. Wood
John A. Paulson School of Engineering and Applied Sciences,
Wyss Institute for Biologically Inspired Engineering,
Harvard University,
Cambridge, MA 02138
e-mail: rjwood@seas.harvard.edu

Flying insects are able to navigate complex and highly dynamic environments, can rapidly change their flight speeds and directions, are robust to environmental disturbances, and are capable of long migratory flights. However, flying robots at similar scales have not yet demonstrated these characteristics autonomously. Recent advances in mesoscale manufacturing, novel actuation, control, and custom integrated circuit (IC) design have enabled the design of insect-scale flapping wing micro air vehicles (MAVs). However, there remain numerous constraints to component technologies—for example, scalable high-energy density power storage—that limit their functionality. This paper highlights the recent developments in the design of small-scale flapping wing MAVs, specifically discussing the various power and actuation technologies selected at various vehicle scales as well as the control architecture and avionics onboard the vehicle. We also outline the challenges associated with creating an integrated insect-scale flapping wing MAV.
[DOI: 10.1115/1.4038795]

1 Introduction

Over the past several decades, unmanned aerial vehicles (UAVs) have found increasing applications in areas including military, media, and entertainment. As these applications evolve and component technologies such as microcontrollers (MCUs), sensors, and energy storage shrink, a new class of UAVs are being developed on much smaller scales. These "micro air vehicles (MAVs)" exist on a scale that is approximately 10 cm to 1 m in characteristic dimension. There are numerous examples as outlined in past MAV reviews [1,2]. As these devices are shrunk further, questions for successful design and operation focus more on materials, mechanics, design, and manufacturing as opposed to control and mission-level programming and planning for larger UAVs.

As the size of the vehicle is decreased, propulsion becomes a key consideration. Fixed wing aircraft at human scales can achieve lift-to-drag ratios in excess of 100. However, as scale is reduced, the Reynolds number is commensurately reduced, resulting in a greater influence of viscous effects that are manifest as increased drag and reduced lift-to-drag ratios. In extreme cases, for devices on the scale of small birds, "nano air vehicles" [3], or insects, "pico air vehicles (PAVs)" [4], fixed wing fluid mechanics becomes impractical as too much energy would be lost to drag at the speeds that would be required to maintain sufficient lift. The same arguments hold for rotary wing vehicles. Quadrotor MAVs exist down to tens of grams (Aerius, Aerix Drones, Fairport, NY); however as size is reduced, the decreasing propulsive efficiency becomes clear in reduced flight times [5]. Furthermore, beyond reduced propulsive efficiency, for insect-scale PAV, there are additional challenges for actuation. Traditional electromagnetic motors are subject to scaling laws that result in degraded performance at reduced sizes [4]. This is caused by unfavorable scaling of surface area to volume, unfavorable scaling of electromagnetic force, limitations on current density, and the need for excessive gearing given the increase in unloaded revolutions per minute (RPM) as size is reduced [6]. In addition, there are significant challenges to manufacturing motors at these scales. Alternative actuation strategies have been explored and will be reviewed in this paper as they pertain to MAV designs.

A bioinspired alternative to traditional propulsion mechanisms is the use of flapping wings. Flapping wing MAVs can overcome some of the challenges discussed earlier by using oscillating actuation in place of rotary actuators and can take advantage of unsteady fluid effects described in the following. However, wing motions can involve several degrees-of-freedom (DOF), creating a challenging design problem for how to generate high-speed, high-efficiency articulating mechanisms at millimeter scales (see Fig. 1 for a model of insect-scale flapping wing MAVs).

One consequence of flapping wings is highly unsteady fluid forces. In contrast to continuously translating or rotating wings, flapping wings experience periodic pressure variations that arise from a number of phenomena. Rapid wing inversions at the end of each half stroke enhance circulation resulting in augmented lift during this phase of the wing cycle [7]. As the wing accelerates into the next half-cycle, it encounters the wake from the previous half-cycle, which can significantly affect flapping kinematics and the corresponding force generation [8]. During the middle of the stroke, the angle of attack—approximately constant during this phase—can greatly exceed angles of attack that would result in stall for conventional aircraft due to leading edge vortex stabilization mechanisms [9]. In some animals and flapping wing MAVs, the wing stroke amplitude can be sufficiently large such that at the end of one or both half-strokes the wings can come in to physical

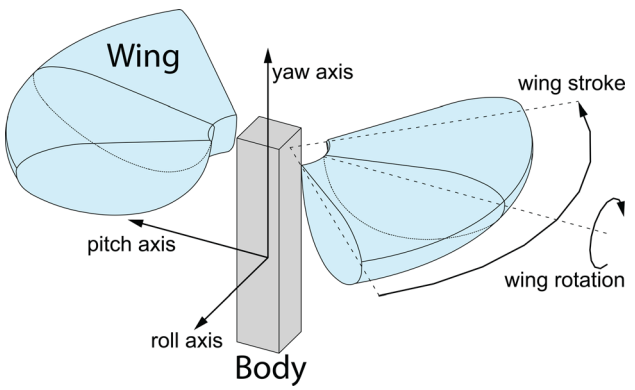

Fig. 1 Parameter definition for insect-scale flapping wing MAV

[1]Corresponding author.
Manuscript received March 19, 2017; final manuscript received December 16, 2017; published online January 18, 2018. Editor: Harry Dankowicz.

contact, resulting in more favorable starting conditions for the vorticity at the start of the next half-cycle [10].

Micro air vehicle designers have sought to navigate the tradeoffs associated with the creation of flapping wing propulsion mechanisms that exploit some or all of these phenomena. For example, mimicking the exact kinematics of an insect species may allow the vehicle to exploit each of these unsteady effects but would potentially require a large number of actuators and a complex transmission mechanism. Furthermore, with respect to control, one critical question is whether body torques are modulated directly by the wings through changes to the nominal wing motions or through ancillary control surfaces. The question of which wing motions to target and how to achieve them, with emphasis on insect-like motions at insect scales, is a key focus of this review.

This review will also describe power and control systems that attempt to mirror some functions of the metabolic and sensorimotor systems in insects. As with the propulsion systems, there are noteworthy tradeoffs in the design of sensing and control electronics that impact energy storage and flight range. For example, the desired level of autonomy—ranging from uncontrolled, passively stable flight to teleoperation to full autonomy—will impose requirements on onboard electronics that will, in turn, also impact overall power consumption and flight duration and range.

Researchers in Ref. [1] provided a review of bird-inspired flapping wing MAV designs, focusing specifically on the mechanics of flight control and the design of the wing and drive mechanisms. That paper discussed vehicles with wingspans in the range from approximately 5–65 cm and body mass range from approximately 1.5–300 g. Here, we discuss a number of vehicles that have been developed since its publication, as well as vehicles that use less traditional actuation strategies. This review primarily focuses on vehicles at a smaller scale, with a wingspan of less than approximately 20 cm and a body mass less than 20 g (see Fig. 2 for the vehicles discussed in this review). As characteristic length decreases, it is necessary to describe alternatives to component technologies relative to larger vehicles, such as alternatives to motors, gears, and rotary bearings, alternative manufacturing methods, as well as alternative methods for lift generation. In addition, we survey vehicles that have achieved varying levels of control autonomy and the necessary avionics at this scale. This review begins with a survey of actuation technologies and power electronics for centimeter-scale flapping wing MAVs in Sec. 2. Section 3 follows with a summary of the control architectures to generate lift and control torques to maintain flight at various scales. Representative examples of centimeter-scale vehicles that have demonstrated autonomy are then discussed in Sec. 4. Finally, the challenges associated with designing power and control architectures for an insect-scale vehicle are discussed in Sec. 5.

2 Actuation and Power Electronics

The physics of scaling dictates that as the characteristic dimension of a device decreases, surface forces, such as friction, electrostatic, and van der Waals, begin to dominate relative to Newtonian forces. This has many practical implications; one of the most relevant is that the use of bearing-based rotary joints becomes inefficient at smaller scales. To overcome frictional losses, the New York University (NYU) Jellyfish Flyer [13] uses short segments of low-friction Teflon tubing as a rotary bearing. At the insect scale, another method to create efficient joints is to embed flexible layers between two rigid links to create compliant flexures. These embedded flexures are used in a number of flapping wing MAVs presented in this paper, including the Carnegie Mellon University (CMU) flapping wing MAVs [12], the electromagnetic flyer [17], the University of California, Berkeley Micromechanical Flying Insect (MFI) [22], the Air Force Research Lab (AFRL) Piezo-Driven flapping wing MAV [20], as well the Harvard RoboBee vehicles [23,24]. The fabrication process to create these composite structures is described in more detail in Ref. [22]. This process was further developed into the "PC-MEMS" process [25] to create complex three-dimensional structures that are used in many of the designs described in detail in the following.

While DC motors are used in the majority of flapping wing MAVs because of their robustness, ease of operation, and ubiquity in macroscale robotics, electromagnetic forces suffer unfavorable scaling at small sizes [26]. Thus, insect-scale robots require nontraditional motors, such as chemical, electrostatic, or piezoelectric, to meet the requirements for power density and bandwidth in these applications [27].

2.1 Motors. As stated earlier, the majority of flapping wing MAVs utilizes DC motors as power actuators. Motors typically operate at low voltages amenable to standard off-the-shelf motor drivers, eliminating the need for complex power electronics. Recent vehicle designs that have utilized electromagnetic motors include the Harvard Robot Moth [11], Aerovironment's Nano-hummingbird [3], the NYU Jellyfish Flyer [13], and the CMU flapping wing MAV [28].

Researchers at CMU [28] integrated a helical spring in parallel to the motor. In this system, energy stored in the spring during a half cycle is released in the subsequent half cycle and assists the motor in reversing the direction of the system inertia. By tuning the spring stiffness so the system resonates at the flapping frequency, the vehicle can save energy by eliminating reactive power needed to oscillate the rotor and wing inertias. This also has the benefit of reducing current spikes by "smoothing" the required motor torque over a period of cyclic motion [29].

2.2 Nontraditional Motor Selection. There are many options for creating the oscillating motions associated with flapping wings. Proper actuator choice must reconcile the specific requirements of the torque, displacement, and flapping frequency with scaling laws that place limits on the performance of the core actuation element. More generally, actuators can be classified based on their force/torque, displacement, bandwidth, mass, and efficiency characteristics. In addition, there are numerous practical constraints that must be considered including ease of manufacture and ease of physical and electrical integration. With respect to the latter, some electrically driven actuators may require high fields. This tradeoff will be discussed in more detail in Sec. 5.1.1.

In Ref. [30], Michelson describes the development of a conceptual reciprocating chemical muscle to power flapping-wing flight of the Entomopter. The reciprocating chemical muscle uses a noncombustive chemical reaction between a monopropellant and an oxidizer. With this reaction, the muscle can create the oscillatory wing stroke motion to generate lift. Additionally, the Central Intelligence Agency developed a dragonfly-inspired flapping wing MAV in the 1970s. The Insectothopter had a miniature fluidic oscillator that controlled the wing stroke motion at a fixed frequency. The excess gas from the chemical reaction was vented out the back of the vehicle creating additional thrust. Video shows that a 1 g prototype vehicle could fly up to 200 m for 60 s [14]. The use of chemical muscles obviates the need for an onboard electrical power supply necessary for conventional actuation technologies but requires a separate electrical system for control and navigation.

Researchers at Shanghai Jiao Tong University have created an insect-scale flapping wing MAV using an oscillating electromagnetic actuator [17]. The vehicle has a mass of 80 mg and a wingspan of 3.5 cm and was manufactured using the Smart Composite Microstructures process described in Ref. [22] and in Sec. 5. The actuator is comprised of a neodymium iron boron magnet attached to a transmission system consisting of two planar four-bars that map actuator motion to the rotational wing stroke motion. The electromagnetic force that acts on the magnet is created by a copper coil attached to the airframe. However, this vehicle consumes approximately 1.2 W of power during flight, which corresponds to a minimum power density of 15 kW/kg (calculated using the mass

of vehicle—no total thrust was reported). The power density of the onboard energy source will be larger than this—the vehicle will need to scale to accommodate the mass of the battery, requiring more power while also increasing the required thrust to accommodate the mass of the battery and drive electronics.

Researchers at the University of Tokyo [16] developed a butterfly-inspired flapping wing MAV using a rubber band as the motor and means of energy storage. The vehicle had a wingspan of approximately 14 cm, a weight of 400 mg, and a flapping frequency of 10 Hz (controlled by the rubber band's thickness and length). The vehicle demonstrated stable forward flight with no active control.

Insects and similar-sized MAVs require relatively high flapping frequencies, often hundreds of hertz [31]. Piezoelectric actuators are typically high bandwidth and numerous motion amplifying mechanisms have been developed to overcome inherent strain limitations, such as benders [32,33] and flextensional actuators [34,35]. Researchers at Vanderbilt University [18] designed a number of vehicles using piezoelectric unimorph actuators to generate wing motions. By using actuators with different excitation frequencies between wings, they created differing wing stroke amplitudes and thus are able to modulate lift bilaterally between vehicle halves. Researchers at CMU also created flapping vehicles with piezoelectric cantilever bimorphs (similar to those described in detail in Ref. [33]); however, these vehicles were not able to achieve sufficient thrust for flight [12]. UC, Berkeley's MFI project attempted to create an insect-scale flapping wing MAV using four piezoelectric cantilever bimorphs [22]. These actuators, two per wing, were mapped to the desired flapping and rotation motions through planar and spherical flexure-based transmission mechanisms [22]. This device was able to demonstrate high wingbeat frequencies and generate lift suitable for takeoff of an insect-scale device [36]. Additionally, researchers at the AFRL created a piezo-driven flapping vehicle [37]. Simulations demonstrated that this vehicle could control horizontal and vertical forces as well as roll and yaw moments with split-cycle wingbeat control. At the millimeter scale, researchers at the ARL built a PiezoMEMS-driven wing which could control wing stroke motion and wing pitch motion independently [21].

3 Mechanisms for Flight Control

The forward-flight capable vehicles discussed in Ref. [1] use multiple control surfaces to generate torques to either stabilize or control the MAV. These include static, rudder, and ruddervator tails, as well as independently controlled wings that can flap or four symmetric clapping wings. At the centimeter scale, we see fewer examples of articulated control surfaces, likely due to the challenges for small-scale actuation.

3.1 Articulated Control Surfaces and Modification of Wing Shape. Recently, researchers at the University of Illinois at Urbana-Champaign have developed the "BatBot" that uses articulated wing joints to actively change wing shape during flight to initiate controlled flight maneuvers [38]. The wing stroke is controlled by a mechanical oscillator that couples the left and right sides. Each wing is individually actuated to allow for asynchronous mediolateral motion. By connecting the three primary revolute joints at the shoulder, elbow, and wrist with rigid links, the robot is able to control the shoulder angle, elbow angle, and wrist angle with one DOF. Given the arrangement of the mechanical skeleton, passive DOFs on the wing tip include flexion–extension, pronation, and abduction–adduction. An additional actuated leg mechanism on each wing allows for control of the trailing edge of the membrane wing, which can increase the angle of attack at the tail. A silicone-based wing membrane adapts to changes in the wing skeleton.

The Nanohummingbird utilizes a string-based flapping mechanism to generate wing stroke motion [3]. In this system, two strings are connected to a crankshaft driven by a central motor.

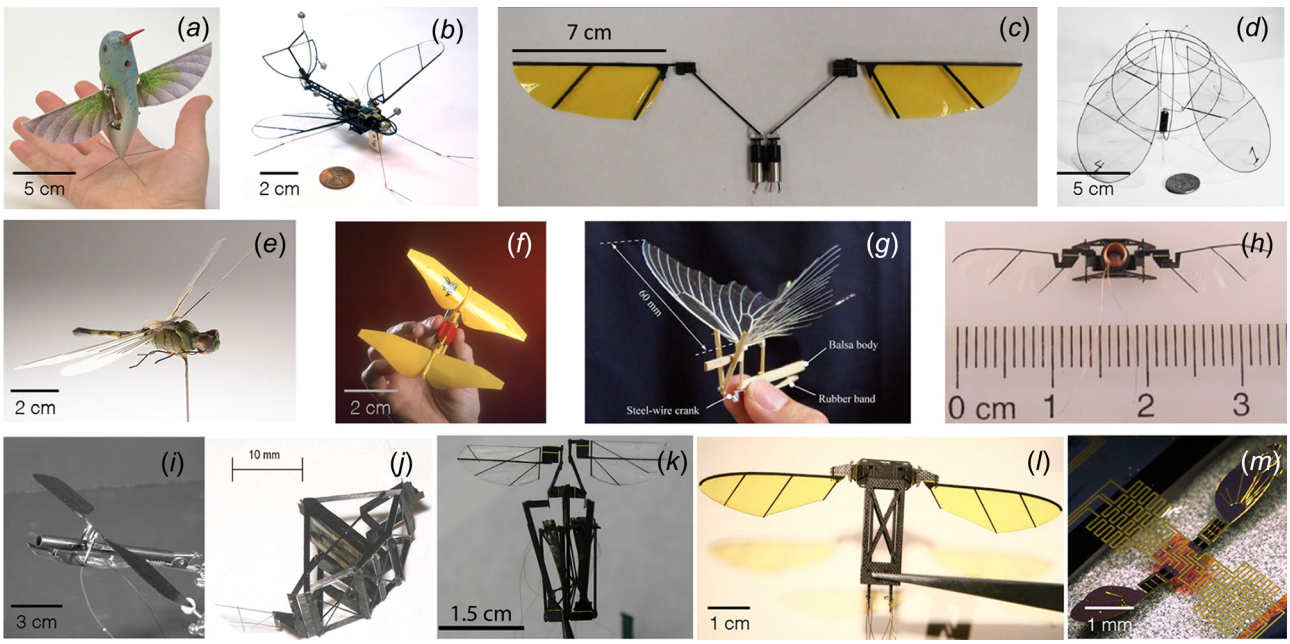

Fig. 2 Representative insect-scale flapping wing MAVs. Top row, traditional motor-driven vehicles: (*a*) aerovironment nano-hummingbird (Image Courtesy of Keennon et al. [3]. Copyright 2012 by Aerovironment, Inc.), (*b*) Harvard Robot Moth [11], (*c*) CMU flapping wing MAV (Reproduced with permission from Hines [12]. Copyright 2014 by Carnegie Mellon University.), (*d*) Jellyfish Flyer [13]. Middle row, nontraditional motor-driven vehicles: (*e*) Central Intelligence Agency insectothopter [14], (*f*) entomopter [15], (*g*) Butterfly-inspired flapping wing MAV (Reproduced with permission from Tanaka and Shimoyama [16]. Copyright 2010 by IOP Publishing.), (*h*) Electromagnetic flapping wing MAV (Reproduced with permission from Zou et al. [17]. Copyright 2016 by IEEE.). Bottom row, Piezo-Driven vehicles: (*i*) Cox Piezo Flyer (Reproduced with permission from Cox et al. [18], Copyright 2002 by SAGE Publications.), (*j*) UC, Berkeley micromechanical flying insect [19], (*k*) CMU Piezo-driven flapping flight platform (Reproduced with permission from Hines [12]. Copyright 2014 by Carnegie Mellon University.), (*l*) AFRL Piezo-driven flapping wing MAV [20], and (*m*) ARMY RESEARCH Lab PiezoMEMS actuated wing design [21].

Each string is attached to two pulleys on the wing hinge flapping axis, such that as the crankshaft turns, the pulleys oscillate to generate the wing motion. Additional strings between the two pulleys maintain the symmetric phasing of the wing motion. This system reduces the mass of the overall control mechanism by eliminating the need for heavier, traditional mechanism designs. The vehicle generates control torques by varying the wing rotation and wing twist. To generate roll torque, the angle of attack varies between the wings to create asymmetric lift forces between the halves. In pitch, the angle of attack is varied between the fore and aft stroke, creating asymmetric lift forces in front or behind the center of mass (COM) of the vehicle. The angle of attack is controlled through wing twisting. During a wing stroke, the wing membrane is able to passively deform, but the root spar of the wing is actively controlled in relation to the leading edge spar, similar to a sail. To generate yaw torque, the angle of attack is varied by controlling the wing rotation amount by actively controlling the stop angle, creating asymmetric drag forces between the wing halves. The final vehicle had a wing span of approximately 16 cm and a total mass of 19 g. The vehicle can hover as well as fly forward at a maximum speed of 6.7 m/s for approximately 4 min.

3.2 Pure Wing Articulation. In the smaller-scale vehicles discussed in this paper, the use of additional control surfaces and actuators becomes impractical given the strict mass and size constraints. The dominant mechanisms for body torque control in insects involves—sometimes subtle—variations to the nominal wing motion, with no active articulation on the wing surface. The MFI uses two independent actuators to actively control wing stroke motion and wing rotation. The flapping motion is generated by mapping the two independent rotations through a spherical five-bar differential transmission. The phasing of the actuators determines the wing stroke and rotation. This vehicle demonstrated sufficient lift to takeoff, but has not demonstrated open-loop flight [36].

To reduce the number of actuators necessary for varying wing morphology, many researchers use a wing hinge that allows the wing to passively pitch due to the inertial and aerodynamic forces on the wing during the wing stroke, eliminating an actuator to control wing rotation. Examples include the Harvard Robot Moth [11], the electromagnetic flyer from Ref. [17], and the CMU vehicles [12]. The wing stroke amplitude and frequency for the Harvard Robot Moth is controlled by a DC motor and transmitted through a crank-slider mechanism to each wing. In previous versions, additional elastic elements were added to the transmission system to store energy, thus decreasing total input power [39]. This vehicle has demonstrated open-loop forward flight through the use of passive stabilization surfaces. Additionally, the electromagnetic flyer in Ref. [17] converts the oscillating motion of the magnet to wing stroke motion through two planar four-bar transmissions. The vehicle demonstrated sufficient thrust-to-weight to take-off on vertical guide rails. The CMU vehicle from Ref. [28] uses the helical spring attached to the output of the motor allows users to vary flapping frequency by adjusting the stiffness of spring. The vehicle has a wingspan of approximately 20 cm, a mass of 2.7 g, and produced a thrust-to-weight ratio of 1.4. Two power actuators are used to power flight and simultaneously generate torques. Roll torque is generated by varying the amplitude of the signal between vehicle halves. The vehicle generates pitch torque by introducing a constant voltage bias to the motor. This is similar to the RoboBee torque generation described in Sec. 5.2.

Researchers at NYU created a flapping wing MAV that employs a flapping motion that opens and closes four wings, resembling a jellyfish. This system has one motor attached to two vertical loops, which attach to an upper loop that acts as a fulcrum. As the motor rotates, the wings are pushed in or pulled out through a system of lightweight links. By tuning the voltage of the motor, the vehicle is able to demonstrate stable upward flight and by increasing the flapping amplitude of one half relative to the other by changing the link lengths, the vehicle can fly in a predetermined direction. This vehicle has also demonstrated successful hovering flight without any external control [13].

4 Control Electronics

Much of the research into flapping-wing robots has focused on the design and construction of the mechanical system to demonstrate open-loop flight ability. Passive mechanisms, such as sails [40] or tails, can act as aerodynamic dampers to stabilize the vehicle during flight. Passive stability can also be built into the design with proper positioning of the wings at a dihedral angle [41] or lowering the COM of the vehicle relative to the wings. Without passive elements, active sensorimotor systems like those found in insects must be developed to stabilize the vehicle and control flight. Vehicles that have demonstrated autonomous flight using onboard control electronics are, notably, the Nanohummingbird and the Delfly [42].

The two-wing, tailless design of the Nanohummingbird creates an attitude instability that requires low latency sensory feedback of the vehicle's orientation to remain in flight. In addition, researchers included an onboard vision system for navigation and obstacle avoidance for future missions (currently no vision processing is completed onboard—information is transmitted to a ground station). The wings of the Delfly II and the Delfly Micro are positioned symmetrically at a positive dihedral angle to allow for passive stability during lateral flight [42]. This relaxes the requirements for onboard sensors, simplifying the control electronics. These vehicles have onboard cameras and transmitters to control flight through teleoperation from a ground station. The Delfly II was also equipped with an onboard barometer to allow for autonomous altitude control.

5 Progress on the RoboBee

The Harvard "RoboBee" project represents a concerted effort to create an autonomous insect-scale flapping wing MAV. The advances of this project in the fabrication of mesoscale devices, manufacturing of highly energy dense actuators, and design of new custom integrated circuits (ICs) have greatly furthered this goal, and are outlined in the following.

The overall design of the RoboBee flight apparatus has been described extensively, for example, in Refs. [4], [43], and [44]. In particular, Whitney et al. described the aeromechanics of the flight apparatus [45] which assumes a rigid flat wing and a passive rotational hinge that enables quasi-static wing pitching (quasi-static relative to the resonant wing stroke motion). This relied on the blade-element method and was further refined by Chen et al. to describe impacts of stroke-pitching phase on vortex creation, shedding, and lift generation [46]. This study also explored wing geometry and scaling in order to match to the actuation and transmission mechanism. More generally, Whitney et al. described tradeoffs in sizing and actuation frequency for flapping wing MAVs [47]—those guidelines can be used to describe the size and specifications for all components of the vehicle's propulsion system, such as the critical choice of actuator type and size.

5.1 Actuation. At the scale and flapping frequency of robotic insects, the composite piezoelectric bimorph actuators optimized for energy density outperform similarly-sized DC motors and other microactuation technologies in terms of bandwidth, efficiency, and power density [33]. The actuators also integrate well into the fabrication process used for creation of the transmission. Wood et al. discuss the optimal geometry and drive configuration of piezoelectric actuators for microrobotic applications, maximizing force, and displacement in low-mass applications [33].

Researchers in Ref. [32] then developed new manufacturing and assembly methods to increase energy and power density of piezoelectric bending actuators by increasing the mechanical flexural strength and dielectric strength. This paper also discussed methods

for mass manufacturing, a step toward making piezoelectric actuators more ubiquitous in flapping wing MAVs. The authors then designed multilayer piezoelectric actuators [48], using four active layers and thinner materials. This lowers the operating voltage, which reduces the complexity of the drive circuitry, minimizing payload, as well as increases efficiency, as efficiency increases with decreasing drive voltage due to losses in the drive stage.

5.1.1 Power Electronics. The primary limitation of piezoelectric actuators are the high drive voltages (150–200 V) required to create the necessary force and displacement to maximize the work that these actuators can perform. However, these fields may be higher than the depoling threshold of the piezoelectric material. Therefore, it is important to drive the bimorph with a unipolar drive signal. Researchers in Ref. [33] describe the drive configurations for a piezoelectric cantilever bimorph that meet these constraints. In "alternating" drive, two unipolar drive stages are connected to the outer electrodes, operated 180 deg out of phase, with a common ground in the center of the electrode. In "simultaneous" drive, a constant high-voltage bias is applied across the actuator and the center electrode is driven with a unipolar drive stage. In the simultaneous drive configuration, a number (n) of actuators can share the high-voltage bias, requiring ($n-1$) fewer drive stages. This reduces the complexity of the power electronics.

There are a number of circuit topologies to create the high-voltage drive signals necessary for RoboBee actuation. Researchers in Ref. [49] created a hybrid boost converter with a cascaded charge pump circuit to create the high-voltage bias line. Researchers in Ref. [50] discuss the design of custom power electronics which consists of two stages—a DC–DC conversion stage to create the high voltage bias line and a drive stage to generate the drive signal for a single actuator. To reduce mass, researchers in Ref. [51] developed a custom power electronics unit which included a tapped-inductor boost converter and a custom 16 mg driver IC that produces two sinusoidal drive signals (one for each wing). The total mass of the power electronics comes to 40 mg.

To increase the efficiency of the power electronics, Lok et al. analyzed the use of the alternating drive configuration to recover unused energy using dynamic common mode adjustment, envelope tracking, and charge sharing, which would result in a 30–47% decrease in power consumption while reducing weight by 37% relative to a version based on discrete components [51].

5.2 Flight Control Through Wing Articulation. Early in the RoboBee project, critical questions were how to design the propulsion system, how to modulate body torques, and how to merge these functions if possible. As described in Sec. 3, it becomes more rare for small-scale vehicles to have independently actuated control surfaces. Instead, all body torques in the RoboBee are generated by modulating the wing kinematics. This bio-inspired approach has taken cues from several orders of insects. For example, the separation of power and control actuators in Refs. [44] and [52] has analogies to the direct and indirect flight muscles in *Dipteran* insects [53], while the independently controlled wings of the Dual Actuator Bee design are reminiscent of *Odonata* (see Fig. 3 for the vehicle generations of the RoboBee project).

Regardless of the actuator and transmission design, and similar to the two-winged, tailless vehicles discussed in Sec. 3, the two wings of the RoboBee are the control surfaces of these vehicles. To execute control maneuvers, the RoboBee generates torques through subtle variations of the wing motion. For each wing, we have control over the wing stroke amplitude, the flapping speed, wing stroke bias (i.e., fore or aft with respect to the COM), as well as the wing pitch angle. The wing stroke motion and flapping frequency are controlled directly through the actuation signal. The passive hinge at the base of the wing controls the wing pitch angle. As flapping speed increases, the inertial and aerodynamic forces on the wing increase and the wing passively pitches due to the compliance of the flexure hinge at the base of the wing and the location of this rotational axis relative to the wing leading edge [43,45]. Resonance is exploited in the system to generate large wing stroke amplitudes and to avoid reactive losses to the inertia of the wing. We generate roll torque by varying the relative wing stroke amplitude, pitch torque by moving the mean stroke angle fore or aft of the COM, and yaw torque by inducing asymmetric drag on the wings (see Fig. 1 for axes definition).

Finio et al. took inspiration from *Drosophilia*, which have antagonistic "indirect" power muscles and a smaller "direct" control muscles that inject directly onto each wing to fine tune the wing motion during flight [53]. Two control actuators were added to the previous Harvard microrobotic fly (HMF) design [43] to tune the transmission ratio between the wing and the power actuator during flight. The vehicle demonstrated open-loop pitch and roll maneuvers [44]; however, these torques were highly coupled and efforts to control the vehicle in flight were unsuccessful.

To reduce the number of actuators, Ma et al. [23] revisited the original HMF design and split the power actuator in two, creating two independent halves, each wing with its own power actuator (see Fig. 4). This design generated decoupled pitch and roll torques due to the decoupling of each half. This vehicle, with a mass of 80 mg and a wingspan of 2.5 cm, demonstrated the first controlled hovering flight of an insect-scale vehicle [23] and has been used as a platform for many of the control and sensing experiments described in the following. This design, however, could not create sufficient yaw torque to control orientation. The vehicle generates yaw torque by creating asymmetric drag forces on the wings by varying the speed of the up and down strokes [55,56]. However, the second-order dynamics of the actuator-transmission-wing system filters inputs to the actuators, hindering yaw torque production by reducing the energy present in higher harmonics of the drive signal [57].

To this end, Teoh et al. created a single power, single control actuator design inspired by the fruit fly (*D. melanoaster*). In this design, the control actuator biases the wing hinge to create asymmetric drag forces on the up and down strokes to generate yaw torque. While this vehicle produced greater yaw torque than previous designs [52], the single power actuator again led to coupling between the two halves and could not produce sufficient pitch and roll torques to control flight. Currently, a new vehicle design is being explored, decoupling the two halves with a single power and single control actuator driving each wing. This design has demonstrated hovering flight and heading control [24]. This vehicle design weighs 110 mg due to the additional mass of the control actuators, which could limit the payload capacity for the control electronics necessary to stabilize the vehicle in flight.

5.2.1 Control Demonstrations. The challenges for successful flight at the insect scale also extend to sensing and control. As the vehicle becomes smaller, the rate of rotational acceleration increases, scaling as l^{-1} [58]. This challenge is compounded by the inherent dynamic instability of hovering wing kinematics [59,60]. Therefore, not only must a flight controller perform continuous corrective maneuvers, but also it must do so with a time delay that is orders of magnitude shorter because of the smaller length scale.

Scaling effects on the flapping dynamics and body dynamics also play a critical role in the operation of the control system. For vehicles the size of the RoboBee, the closed-loop body dynamics are approximately an order of magnitude slower than the wingbeat frequency. This implies that control corrections to the wing motions can happen over several wingbeats. These two regimes (body and wing dynamics) converge at larger scales, requiring control on a per-wing-stroke basis.

Researchers have demonstrated a number of controlled flight experiments to demonstrate the vehicle's maneuverability. From an integration perspective, these controllers must be minimally computationally expensive while also being sufficient to perform the desired task. The simplest demonstration of controlled flight

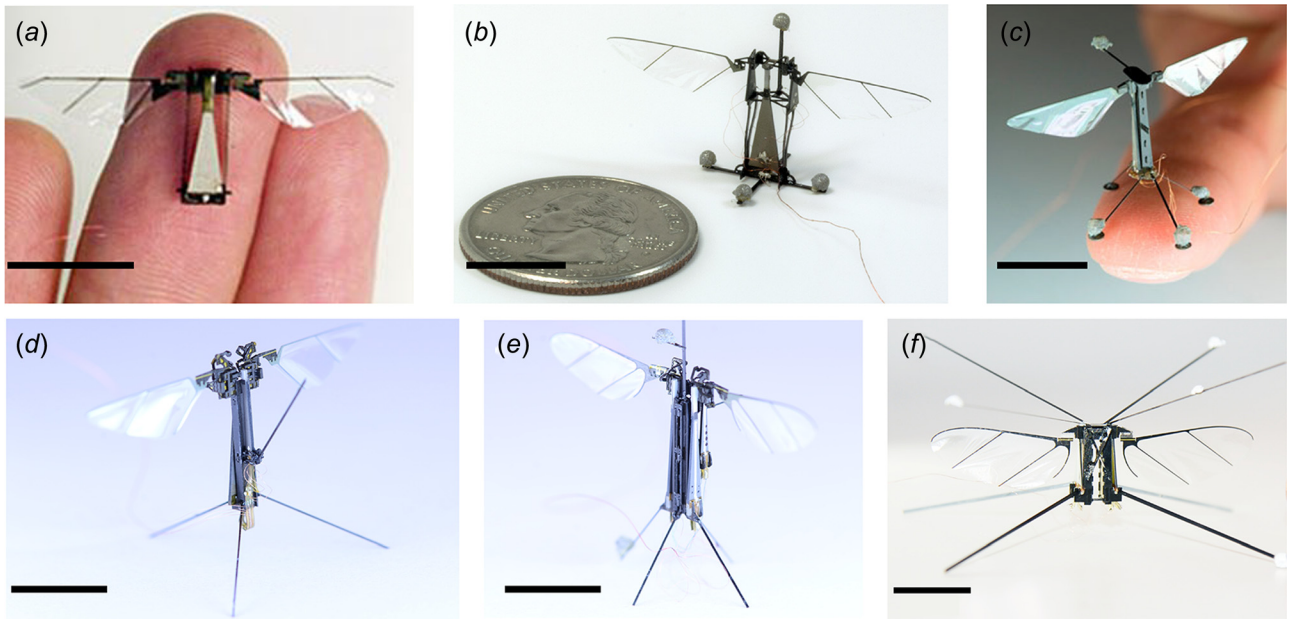

Fig. 3 Generations of the RoboBee. All vehicles designed and manufactured using the SCM [22] and PC-MEMS [25] processes. Each vehicle is actuated using piezoelectric bimorph cantilever actuators. (*a*) The "HMF," with one power actuator and coupled transmission system, demonstrated successful takeoff but without a means for torque generation [43]. (*b*) The first generation RoboBee contained one power actuator and two smaller control actuators. This demonstrated successful torque generation and open-loop flight [44]. (*c*) The "dual actuator bee" contains two power actuators and was the first insect-scale device to achieve controlled flight [23]. (*d*) In an attempt to control yaw torques, the "angle of attack bee" consisted of one power and one control actuator that modulated an angle of attack bias on the wing hinge [52]. (*e*) The subsequent "quad actuator bee" was able to successfully control flight and heading maneuvers. (*f*) The "big bee" is a scaled-up version of the dual actuator bee to meet mass requirements of future onboard control electronics [54]. All scale bars are 1 cm.

was in Ref. [61], where the addition of a passive mechanism mitigated the need for an active controller; however, it greatly reduced the vehicle's maneuverability. The first demonstration of controlled hovering flight used an adaptive controller to perform attitude stabilization and control lateral position and altitude to track a desired trajectory [62]. An iterative learning control algorithm was then developed to allow the vehicle to perform aggressive maneuvers such as perching on a vertical surface [63]. Researchers have also developed computationally inexpensive controllers. Using a model-free approach, multiple proportional–integral–derivative control loops are able to stabilize the vehicle during flight [64]. While previous controllers performed feedback at a rate of 5–10 kHz, recently, researchers experimentally determined that the control loop can control hovering flight (as in Ref. [64]) at frequencies of 250 Hz. This provides the potential for general purpose MCUs to be sufficient to stabilize flight and perform simple maneuvers.

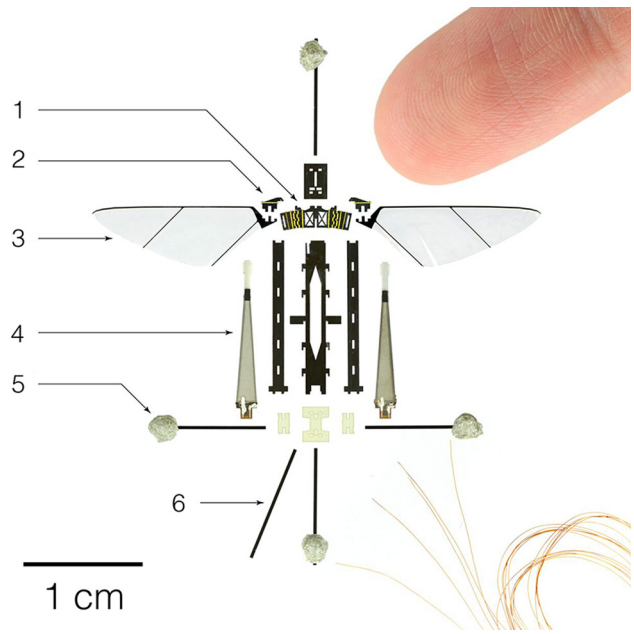

Fig. 4 Components of the dual actuator bee [23]. (1) Transmission, (2) wing hinge, (3) wing, (4) actuator, (5) reflective marker for motion capture tracking, and (6) leg. All remaining components are part of the robot's airframe.

5.3 Control Electronics. All of the controlled flight experiments listed earlier were performed inside a motion capture arena, constrained to a flight volume of approximately one cubic foot. An external computer was used to compute the updated control parameters and generate new drive signals, which are supplied through thin wires to the vehicle's actuators. To render the vehicle autonomous, we must integrate onboard sensors, an MCU, and power electronics (see Fig. 5). An onboard MCU must read onboard sensor information, compute the vehicle's state and update controller commands, as well as generate updated drive signals to interface with the onboard power electronics. This MCU must meet the strict mass and power requirements of the vehicle, eliminating the majority of off-the-shelf MCUs. These MCUs must also compute control commands and generate drive signals for the power electronics with a clock frequency of 60 MHz [65].

To meet these demands, researchers have created a custom "brain" IC with a mass of 6 mg. This chip contains a 32-bit ARM Cortex-M0; four dedicated hardware accelerators (custom circuits that perform single functions with high speed and efficiency), one for image processing, one for estimating rotations, one for body control (process sensory information, update the state estimate, and determine the necessary torque command to stabilize flight), and one for actuator control (convert the torque command to drive

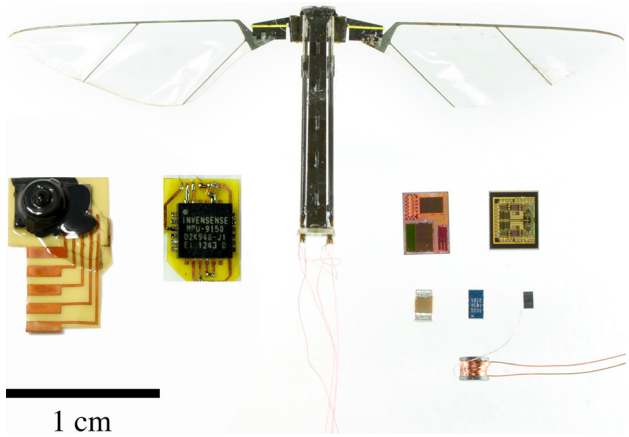

Fig. 5 Electrical components of the RoboBee. Left: optic flow sensor, gyroscope. Right: "brain" IC, "power" IC, DC–DC converter discrete components.

signals); I2C, SPI, and GPIO buses; four ADC channels; and an internal voltage regulator to reduce peripheral components onboard the vehicle [65]. This IC has demonstrated sufficient performance to meet the real-time demands of an autonomous flight using simulated flight data and is currently being migrated onboard the vehicle (see Fig. 6 for control and power schematic).

In addition to custom MCUs, researchers have investigated many sensors that meet the low mass, power, and latency requirements of the vehicle and have demonstrated their use in flight. These sensors include an off-the-shelf gyroscope [66], magnetometer [67], and custom ocelli [68] to stabilize the vehicle's attitude; as well as an off-the-shelf infrared time-of-flight sensor [69] and a custom optic flow sensor [70] to estimate the vehicle's altitude (see Table 1 for mass and power requirements of these components).

To increase payload capacity to accommodate these electrical components, Jafferis et al. created a nonlinear resonance model for under-actuated flapping wing MAVs with passively rotating wing hinges, like the RoboBee [71]. With this model, they determined an optimal pitch angle of 70 deg, and a narrow force window to exploit resonance, increasing the vehicle's payload from 40 mg to 170 mg. In addition, Ma et al. created a design methodology to further scale the vehicle to meet the payload requirements of onboard power electronics and energy storage [54].

5.4 Future Directions. While there have been significant breakthroughs in the manufacturing, control, and actuation of insect-scale flapping wing MAVs, significant research needs to be conducted to integrate the control electronics onto an autonomous vehicle. First, we must determine the minimum number of sensors necessary to stabilize flight. Additional sensors (such as vision) may be needed for various applications. From this, we must determine the minimum sensor latency for adequate state estimation in free flight to determine the minimum computational expense (e.g., floating point operations per second or similar). We must also determine the minimum control requirements to both stabilize the vehicle and have it navigate in the environment. This will help determine the minimum number of instructions that a MCU will need to perform.

The most significant limitation in creating an autonomous insect-scale flapping wing MAV is an onboard power source that meets the stringent mass and size requirements while having sufficient energy density. Current options that meet these requirements include electrochemical and solar. In Ref. [72], researchers performed a system-level optimization on the energetics of flapping-wing flight motivated by maximizing flight time, specifically looking at design parameters such as payload mass, battery energy density, actuator energy density, and power electronics efficiency.

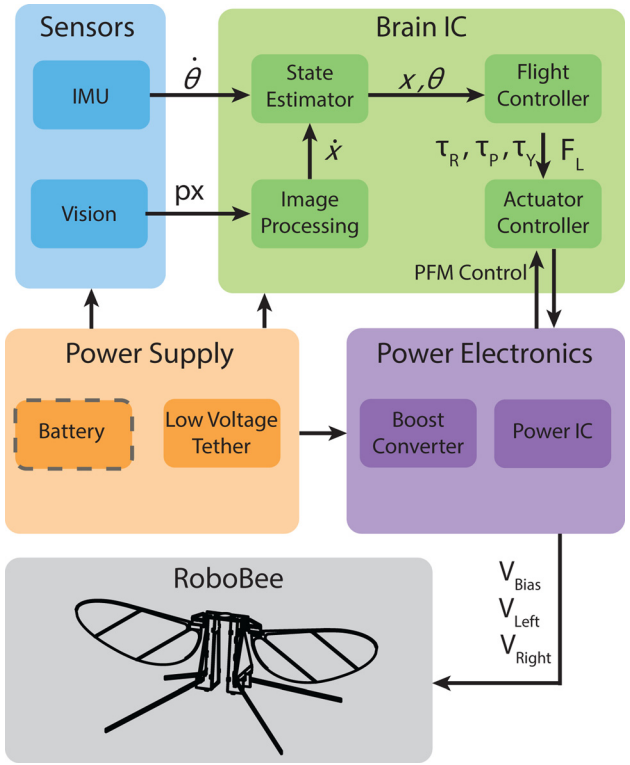

Fig. 6 Control and power schematic of an autonomous RoboBee. The IMU and vision sensors measure the vehicle's state and communicate with the brain IC. The brain IC has a dedicated accelerator to read the pixels from the vision sensor and use optic flow algorithms to determine the vehicle's velocity. This measurement is then used to compute the vehicle's state using another dedicated accelerator. The flight controller takes the vehicle's state and computes the necessary torques. An actuator controller uses these torques to modify the pulse signals to control the power IC and boost converter. The drive signals are sent to the RoboBee. Power will first be supplied through a low voltage tether to be replaced with a battery in the future.

This optimization estimates vehicle size and flapping frequency as well as the mass fraction of an onboard battery. Given the current state of the RoboBee project and using this framework, we estimate that a power-autonomous vehicle will consume 400 mW during hovering flight and can accommodate a battery mass no more than 100 mg.

Commercial lithium polymer and lithium ion batteries are the most commonly used energy storage devices for modern robots. However, there is a dearth of batteries appropriate for the scale of the RoboBee. Batteries produced by FullRiver contain near constant power density (on the order of 1–3 W/g) as the mass scales through three orders of magnitude (0.4–100 g). However, these batteries do not meet the mass requirements of the RoboBee, with the smallest being 4× larger than the target battery payload. Recent work in lithium polymer batteries has demonstrated the

Table 1 Mass and power requirements of the electrical system of the RoboBee

Component	Mass (mg)	Power (mW)
Actuators [54]	196	80
IMU (MPU6500)	15	10
Vision (WhiteOak)	17	10
Brain IC [65]	6	48
Power IC [51]	16	90
Boost converter	50	200

development of a number of microbatteries at the millimeter scale (see Refs. [73] and [74] for a review). For example, Lai et al. [75] created a microbattery with a volume of 6 mm^3 and a maximum dimension of 3 mm with a power density of 150–200 WL^{-1}. Assuming a density of approximately 2 g/cm^3, this would provide 75–100 mW/g.

Solar cells are also a viable option. Recent work has demonstrated their effectiveness on a 3 g autonomous legged microrobot [76]. These cells (epitaxial lift-off solar cells 1-6615-8, MicroLink Devices, Niles, IL) weigh 10 mg per cell and have a 30% efficiency, providing 7.5 mW per cell in 1Sun (1000 Wm^{-2}).

Moving forward, further investigation into the integration of mechanical and electrical systems to create an autonomous insect-scale MAV is required. There has been tremendous progress in the conceptual vehicle design and component-level design, but emphasis on full vehicle integration and associated tradeoffs is needed to realize fully autonomous PAVs. Once this is achieved, the field can move forward to begin taking advantage of the past decades worth of work on aggressive control methods for larger-scale MAVs.

6 Conclusions

This paper has presented a summary of power and control architectures, including propulsive mechanisms, for insect-scale flapping wing MAVs. Power architectures for centimeter-scale vehicles were classified into various actuation technologies available at that scale. We discussed the propulsive mechanisms of these vehicles, which rely on slight modifications to nominal wing motion, rather than articulated control surfaces present in larger UAVs. Due to the stringent payload capacity, there are only two representative examples of vehicles at this scale that have demonstrated any level of control during flight. We then outlined recent advances and current challenges associated with creating an autonomous insect-scale MAV.

In the design of autonomous insect-scale flapping wing MAVs, there are inherent tradeoffs associated with actuator, control, and propulsion methodologies. To design a vehicle at this scale, it is important to understand the different technologies and their implications for power consumption, flight time, and range. This review has summarized the differing designs of insect-scale flapping wing MAVs and explored the advantages and disadvantages of using various actuation, propulsive mechanisms, control methodologies, as well as onboard control and power electronics.

Due to the physics of scaling, actuation for insect-scale MAVs is confined to nontraditional actuation technologies, such as chemical muscles, custom electromagnetic actuators, and piezoelectric actuators. Electromagnetic actuators have a low input voltage but high power consumption; in comparison, piezoelectric actuators require high input voltages and additional payload for high-voltage power electronics but lower power consumption. This analysis was extended to flapping wing propulsion and the desired wing motions. While articulated control surfaces on the wings could allow the vehicle to mimic kinematics of a biological counterpart, the additional actuators and mechanisms may not meet the mass and power requirements of the vehicle. Additionally, many designers have chosen passive elements, such as wing hinges, to further reduce the number of actuators. The level of autonomy and maneuverability required for these vehicles also dictated the complexity of onboard avionics and their power consumption. These tradeoffs were then explored in the insect-scale RoboBee, where the development of custom manufacturing, actuation, control, and electronics were necessary to meet the strict mass and power requirements of the vehicle.

Acknowledgment

This work is supported by the Wyss Institute for Biologically Inspired Engineering. Any opinions, findings, conclusions, or recommendations expressed in this material are those of the authors and do not necessarily reflect the views of the National Science Foundation.

Funding Data

- National Science Foundation (Award No. IIS-1514306).

References

[1] Gerdes, J. W., Gupta, S. K., and Wilkerson, S. A., 2012, "A Review of Bird-Inspired Flapping Wing Miniature Air Vehicle Designs," ASME J. Mech. Rob., **4**(2), p. 021003.
[2] Liu, H., Ravi, S., Kolomenskiy, D., and Tanaka, H., 2016, "Biomechanics and Biomimetics in Insect-Inspired Flight Systems," Phil. Trans. R. Soc. B, **371**(1704), p. 20150390.
[3] Keennon, M., Klingebiel, K., and Won, H., 2012, "Development of the Nano Hummingbird: A Tailless Flapping Wing Micro Air Vehicle," AIAA Paper No. 2012-0588.
[4] Wood, R. J., Finio, B., Karpelson, M., Ma, K., Pérez-Arancibia, N. O., Sreetharan, P. S., Tanaka, H., and Whitney, J. P., 2012, "Progress on Picoair Vehicles," Int. J. Rob. Res., **31**(11), pp. 1292–1302.
[5] Floreano, D., and Wood, R. J., 2015, "Science, Technology and the Future of Small Autonomous Drones," Nature, **521**(7553), pp. 460–466.
[6] Trimmer, W. S., 1989, "Microrobots and Micromechanical Systems," Sens. Actuators, **19**(3), pp. 267–287.
[7] Dickinson, M. H., Lehmann, F.-O., and Sane, S. P., 1999, "Wing Rotation and the Aerodynamic Basis of Insect Flight," Science, **284**(5422), pp. 1954–1960.
[8] Alben, S., and Shelley, M., 2005, "Coherent Locomotion as an Attracting State for a Free Flapping Body," Proc. Natl. Acad. Sci. U.S.A., **102**(32), pp. 11163–11166.
[9] Lentink, D., and Dickinson, M. H., 2009, "Rotational Accelerations Stabilize Leading Edge Vortices on Revolving Fly Wings," J. Exp. Biol., **212**(16), pp. 2705–2719.
[10] Miller, L. A., and Peskin, C. S., 2009, "Flexible Clap and Fling in Tiny Insect Flight," J. Exp. Biol., **212**(19), pp. 3076–3090.
[11] Rosen, M. H., le Pivain, G., Sahai, R., Jafferis, N. T., and Wood, R. J., 2016, "Development of a 3.2 g Untethered Flapping-Wing Platform for Flight Energetics and Control Experiments," IEEE International Conference on Robotics and Automation (ICRA), Stockholm, Sweden, May 16–21, pp. 3227–3233.
[12] Hines, L., 2014, "Design and Control of a Flapping Flight Micro Aerial Vehicle," Ph.D. thesis, Carnegie Mellon University, Pittsburgh, PA.
[13] Ristroph, L., and Childress, S., 2014, "Stable Hovering of a Jellyfish-like Flying Machine," J. R. Soc. Interface, **11**(92), p. 20130992.
[14] Weiss, R., 2007, "Dragonfly or Insect Spy? Scientists at Work on Robobugs," Washington Post Company, Washington, DC, accessed Dec. 28, 2017, http://www.washingtonpost.com/wp-dyn/content/article/2007/10/08/AR2007100801434.html
[15] Colozza, A., Michelson, R., and Naqvi, M., 2002, "Planetary Exploration Using Biomimetics-An Entomopter for Flight on Mars," NASA Institute for Advanced Concepts Project, Ohio Aerospace Institute (OAI), Cleveland, OH, Report No. NAS5-98051.
[16] Tanaka, H., and Shimoyama, I., 2010, "Forward Flight of Swallowtail Butterfly With Simple Flapping Motion," Bioinspiration Biomimetics, **5**(2), p. 026003.
[17] Zou, Y., Zhang, W., and Zhang, Z., 2016, "Liftoff of an Electromagnetically Driven Insect-Inspired Flapping-Wing Robot," IEEE Trans. Rob., **32**(5), pp. 1285–1289.
[18] Cox, A., Monopoli, D., Cveticanin, D., Goldfarb, M., and Garcia, E., 2002, "The Development of Elastodynamic Components for Piezoelectrically Actuated Flapping Micro-Air Vehicles," J. Intell. Mater. Syst. Struct., **13**(9), pp. 611–615.
[19] Steltz, E., Wood, R. J., Avadhanula, S., and Fearing, R. S., 2005, "Characterization of the Micromechanical Flying Insect by Optical Position Sensing," IEEE International Conference on, Robotics and Automation (ICRA), Barcelona, Spain, Apr. 18–22, pp. 1252–1257.
[20] Anderson, M. L., 2011, "Design and Control of Flapping Wing Micro Air Vehicles," Ph.D. thesis, Air Force Institute of Technology, Wright-Patterson Air Force Base, OH.
[21] Smith, G. L., Pulskamp, J. S., Sanchez, L. M., Potrepka, D. M., Proie, R. M., Ivanov, T. G., Rudy, R. Q., Nothwang, W. D., Bedair, S. S., Meyer, C. D., and Polcawich, R. G., 2012, "PZT-Based Piezoelectric MEMS Technology," J. Am. Ceram. Soc., **95**(6), pp. 1777–1792.
[22] Wood, R., Avadhanula, S., Sahai, R., Steltz, E., and Fearing, R., 2008, "Microrobot Design Using Fiber Reinforced Composites," ASME J. Mech. Des., **130**(5), p. 052304.
[23] Ma, K. Y., Chirarattananon, P., Fuller, S. B., and Wood, R. J., 2013, "Controlled Flight of a Biologically Inspired, Insect-Scale Robot," Science, **340**(6132), pp. 603–607.
[24] Teoh, Z. E., 2015, "Design of Hybrid Passive and Active Mechanisms for Control of Insect-Scale Flapping-Wing Robots," Ph.D. thesis, Harvard University, Cambridge, MA.
[25] Sreetharan, P. S., Whitney, J. P., Strauss, M. D., and Wood, R. J., 2012, "Monolithic Fabrication of Millimeter-Scale Machines," J. Micromech. Microeng., **22**(5), p. 055027.
[26] Trimmer, W., and Jebens, R., 1989, "Actuators for Micro Robots," IEEE International Conference on Robotics and Automation (ICRA), Scottsdale, AZ, May 14–19, pp. 1547–1552.
[27] Karpelson, M., Wei, G.-Y., and Wood, R. J., 2008, "A Review of Actuation and Power Electronics Options for Flapping-Wing Robotic Insects," IEEE

International Conference on Robotics and Automation (ICRA), Pasadena, CA, May 19–23, pp. 779–786.
[28] Hines, L., Campolo, D., and Sitti, M., 2014, "Liftoff of a Motor-Driven, Flapping-Wing Microaerial Vehicle Capable of Resonance," IEEE Trans. Rob., **30**(1), pp. 220–232.
[29] Baek, S. S., Ma, K. Y., and Fearing, R. S., 2009, "Efficient Resonant Drive of Flapping-Wing Robots," IEEE/RSJ International Conference on Intelligent Robots and Systems (IROS), St. Louis, MO, Oct. 10–15, pp. 2854–2860.
[30] Michelson, R. C., and Reece, S., 1998, "Update on Flapping Wing Micro Air Vehicle Research-Ongoing Work to Develop a Flapping Wing, Crawling 'Entomopter'," 13th Bristol International RPV Conference, Bristol, UK, Mar. 30–Apr. 1, p. 11.
[31] Dudley, R., 2002, *The Biomechanics of Insect Flight: Form, Function, Evolution*, Princeton University Press, Princeton, NJ.
[32] Jafferis, N. T., Smith, M. J., and Wood, R. J., 2015, "Design and Manufacturing Rules for Maximizing the Performance of Polycrystalline Piezoelectric Bending Actuators," Smart Mater. Struct., **24**(6), p. 065023.
[33] Wood, R., Steltz, E., and Fearing, R., 2005, "Optimal Energy Density Piezoelectric Bending Actuators," Sens. Actuators A: Phys., **119**(2), pp. 476–488.
[34] Newnham, R., Dogan, A., Xu, Q., Onitsuka, K., and Yoshikawa, S., 1993, "Flextensional 'Moonie' Actuators," IEEE Ultrasonics Symposium, Baltimore, MD, Oct. 31–Nov. 3, pp. 509–513.
[35] York, P., and Wood, R., 2017, "A Geometrically-Amplified In-Plane Piezoelectric Actuator for Mesoscale Robotic Systems," IEEE International Conference on Robotics and Automation (ICRA), Singapore, May 29–June 3, pp. 1263–1268.
[36] Steltz, E., Avadhanula, S., and Fearing, R. S., 2007, "High Lift Force With 275 Hz Wing Beat in MFI," IEEE/RSJ International Conference on Intelligent Robots and Systems (IROS), San Diego, CA, Oct. 29–Nov. 2, pp. 3987–3992.
[37] Doman, D. B., Oppenheimer, M. W., and Sigthorsson, D. O., 2010, "Wingbeat Shape Modulation for Flapping-Wing Micro-Air-Vehicle Control During Hover," J. Guidance, Control, Dyn., **33**(3), pp. 724–739.
[38] Ramezani, A., Chung, S.-J., and Hutchinson, S., 2017, "A Biomimetic Robotic Platform to Study Flight Specializations of Bats," Sci. Rob., **2**(3), p. eaal2505.
[39] Sahai, R., Galloway, K. C., and Wood, R. J., 2013, "Elastic Element Integration for Improved Flapping-Wing Micro Air Vehicle Performance," IEEE Trans. Rob., **29**(1), pp. 32–41.
[40] Van Breugel, F., Regan, W., and Lipson, H., 2008, "From Insects to Machines," IEEE Rob. Autom. Mag., **15**(4), pp. 68–74.
[41] Koopmans, J., Tijmons, S., De Wagter, C., and de Croon, G., 2015, "Passively Stable Flapping Flight From Hover to Fast Forward Through Shift in Wing Position," Int. J. Micro Air Veh., **7**(4), pp. 407–418.
[42] De Croon, G., De Clercq, K., Ruijsink, R., Remes, B., and De Wagter, C., 2009, "Design, Aerodynamics, and Vision-Based Control of the Delfly," Int. J. Micro Air Veh., **1**(2), pp. 71–97.
[43] Wood, R. J., 2007, "Liftoff of a 60 mg Flapping-Wing Mav," IEEE/RSJ International Conference on Intelligent Robots and Systems (IROS), San Diego, CA, Oct. 29–Nov. 2, pp. 1889–1894.
[44] Finio, B. M., and Wood, R. J., 2012, "Open-Loop Roll, Pitch and Yaw Torques for a Robotic Bee," IEEE/RSJ International Conference on Intelligent Robots and Systems (IROS), Vilamoura, Portugal, Oct. 7–12, pp. 113–119.
[45] Whitney, J., and Wood, R., 2010, "Aeromechanics of Passive Rotation in Flapping Flight," J. Fluid Mech., **660**, pp. 197–220.
[46] Chen, Y., Ma, K., and Wood, R. J., 2016, "Influence of Wing Morphological and Inertial Parameters on Flapping Flight Performance," IEEE/RSJ International Conference on Intelligent Robots and Systems (IROS), Daejeon, South Korea, Oct. 9–14, pp. 2329–2336.
[47] Whitney, J., and Wood, R., 2012, "Conceptual Design of Flapping-Wing Micro Air Vehicles," Bioinspiration Biomimetics, **7**(3), p. 036001.
[48] Jafferis, N. T., Lok, M., Winey, N., Wei, G.-Y., and Wood, R. J., 2016, "Multilayer Laminated Piezoelectric Bending Actuators: Design and Manufacturing for Optimum Power Density and Efficiency," Smart Mater. Struct., **25**(5), p. 055033.
[49] Steltz, E., Seeman, M., Avadhanula, S., and Fearing, R. S., 2006, "Power Electronics Design Choice for Piezoelectric Microrobots," IEEE/RSJ International Conference on Intelligent Robots and Systems (IROS), Beijing, China, Oct. 9–15, pp. 1322–1328.
[50] Karpelson, M., Wei, G.-Y., and Wood, R. J., 2012, "Driving High Voltage Piezoelectric Actuators in Microrobotic Applications," Sens. Actuators A: Phys., **176**, pp. 78–89.
[51] Lok, M., Zhang, X., Helbling, E. F., Wood, R., Brooks, D., and Wei, G.-Y., 2015, "A Power Electronics Unit to Drive Piezoelectric Actuators for Flying Microrobots," IEEE Custom Integrated Circuits Conference (CICC), San Jose, CA, Sept. 28–30, pp. 1–4.
[52] Teoh, Z. E., and Wood, R. J., 2014, "A Bioinspired Approach to Torque Control in an Insect-Sized Flapping-Wing Robot," Fifth IEEE RAS & EMBS International Conference on Biomedical Robotics and Biomechatronics, Sao Paulo, Brazil, Aug. 12–15, pp. 911–917.
[53] Dickinson, M. H., and Tu, M. S., 1997, "The Function of Dipteran Flight Muscle," Comp. Biochem. Physiol. Part A: Physiol., **116**(3), pp. 223–238.
[54] Ma, K. Y., Chirarattananon, P., and Wood, R. J., 2015, "Design and Fabrication of an Insect-Scale Flying Robot for Control Autonomy," IEEE/RSJ International Conference on Intelligent Robots and Systems (IROS), Hamburg, Germany, Sept. 28–Oct. 2, pp. 1558–1564.
[55] Oppenheimer, M., Doman, D., and Sigthorsson, D., 2010, "Dynamics and Control of a Biomimetic Vehicle Using Biased Wingbeat Forcing Functions—Part I: Aerodynamic Model," AIAA Paper No. 2010-1023.
[56] Doman, D., Oppenheimer, M., and Sigthorsson, D., 2010, "Dynamics and Control of a Biomimetic Vehicle Using Biased Wingbeat Forcing Functions—Part II: Controller," AIAA Paper No. 2010-1024.
[57] Gravish, N., and Wood, R. J., 2016, "Anomalous Yaw Torque Generation From Passively Pitching Wings," IEEE International Conference on Robotics and Automation (ICRA), Stockholm, Sweden, May 16–21, pp. 3282–3287.
[58] Kumar, V., and Michael, N., 2012, "Opportunities and Challenges With Autonomous Micro Aerial Vehicles," Int. J. Rob. Res., **31**(11), pp. 1279–1291.
[59] Faruque, I., and Humbert, J. S., 2010, "Dipteran Insect Flight Dynamics—Part 1: Longitudinal Motion About Hover," J. Theor. Biol., **264**(2), pp. 538–552.
[60] Ristroph, L., Ristroph, G., Morozova, S., Bergou, A. J., Chang, S., Guckenheimer, J., Wang, Z. J., and Cohen, I., 2013, "Active and Passive Stabilization of Body Pitch in Insect Flight," J. R. Soc. Interface, **10**(85), p. 20130237.
[61] Teoh, Z. E., Fuller, S. B., Chirarattananon, P., Prez-Arancibia, N., Greenberg, J. D., and Wood, R. J., 2012, "A Hovering Flapping-Wing Microrobot With Altitude Control and Passive Upright Stability," IEEE/RSJ International Conference on Intelligent Robots and Systems (IROS), Vilamoura, Portugal, Oct. 7–12, pp. 3209–3216.
[62] Chirarattananon, P., Ma, K. Y., and Wood, R. J., 2014, "Adaptive Control of a Millimeter-Scale Flapping-Wing Robot," Bioinspiration Biomimetics, **9**(2), p. 025004.
[63] Chirarattananon, P., Ma, K. Y., and Wood, R. J., 2016, "Perching With a Robotic Insect Using Adaptive Tracking Control and Iterative Learning Control," Int. J. Rob. Res., **35**(10), pp. 1185–1206.
[64] Pérez-Arancibia, N. O., Pierre-Emile, J. D., Ma, K. Y., and Wood, R. J., 2015, "Model-Free Control of a Hovering Flapping-Wing Microrobot," J. Intell. Rob. Syst., **77**(1), pp. 95–111.
[65] Zhang, X., Lok, M., Tong, T., Chaput, S., Lee, S. K., Reagen, B., Lee, H., Brooks, D., and Wei, G.-Y., 2015, "A Multi-Chip System Optimized for Insect-Scale Flapping-Wing Robots," Symposium on VLSI Circuits (VLSI Circuits), Kyoto, Japan, June 17–19, pp. C152–C153.
[66] Fuller, S. B., Helbling, E. F., Chirarattananon, P., and Wood, R. J., 2014, "Using a MEMS Gyroscope to Stabilize the Attitude of a Fly-Sized Hovering Robot," International Micro Air Vehicle Conference and Competition (IMAV), Delft University of Technology, Delft, The Netherlands, Aug. 12–15, pp. 102–109.
[67] Helbling, E. F., Fuller, S. B., and Wood, R. J., 2014, "Pitch and Yaw Control of a Robotic Insect Using an Onboard Magnetometer," IEEE International Conference on Robotics and Automation (ICRA), Hong Kong, China, May 31–June 7, pp. 5516–5522.
[68] Fuller, S. B., Karpelson, M., Censi, A., Ma, K. Y., and Wood, R. J., 2014, "Controlling Free Flight of a Robotic Fly Using an Onboard Vision Sensor Inspired by Insect Ocelli," J. R. Soc. Interface, **11**(97), p. 20140281.
[69] Helbling, E. F., Fuller, S. B., and Wood, R. J., 2017, "Altitude Estimation and Control of an Insect-Scale Robot With an Onboard Proximity Sensor," *Robotics Research*, Springer, Cham, Switzerland, pp. 57–69.
[70] Duhamel, P.-E. J., Pérez-Arancibia, N. O., Barrows, G. L., and Wood, R. J., 2013, "Biologically Inspired Optical-Flow Sensing for Altitude Control of Flapping-Wing Microrobots," IEEE/ASME Trans. Mechatronics, **18**(2), pp. 556–568.
[71] Jafferis, N. T., Graule, M. A., and Wood, R. J., 2016, "Non-Linear Resonance Modeling and System Design Improvements for Underactuated Flapping-Wing Vehicles," IEEE International Conference on Robotics and Automation (ICRA), Stockholm, Sweden, May 16–21, pp. 3234–3241.
[72] Karpelson, M., Whitney, J. P., Wei, G.-Y., and Wood, R. J., 2010, "Energetics of Flapping-Wing Robotic Insects: Towards Autonomous Hovering Flight," IEEE/RSJ International Conference on Intelligent Robots and Systems (IROS), Taipei, Taiwan, Oct. 18–22, pp. 1630–1637.
[73] Wang, Y., Liu, B., Li, Q., Cartmell, S., Ferrara, S., Deng, Z. D., and Xiao, J., 2015, "Lithium and Lithium Ion Batteries for Applications in Microelectronic Devices: A Review," J. Power Sources, **286**, pp. 330–345.
[74] Ferrari, S., Loveridge, M., Beattie, S. D., Jahn, M., Dashwood, R. J., and Bhagat, R., 2015, "Latest Advances in the Manufacturing of 3D Rechargeable Lithium Microbatteries," J. Power Sources, **286**, pp. 25–46.
[75] Lai, W., Erdonmez, C. K., Marinis, T. F., Bjune, C. K., Dudney, N. J., Xu, F., Wartena, R., and Chiang, Y.-M., 2010, "Ultrahigh-Energy-Density Microbatteries Enabled by New Electrode Architecture and Micropackaging Design," Adv. Mater., **22**(20), pp. E139–E144.
[76] Brühwiler, R., Goldberg, B., Doshi, N., Ozcan, O., Jafferis, N., Karpelson, M., and Wood, R. J., 2015, "Feedback Control of a Legged Microrobot With On-Board Sensing," IEEE/RSJ International Conference on Intelligent Robots and Systems (IROS), Hamburg, Germany, Sept. 28–Oct. 2, pp. 5727–5733.